International Journal of Oceans and Oceanography
ISSN 0973-2667 Volume 13, Number 2 (2019), pp. 395-426

http://www.ripublication.com

Seasonal Variations of Plankton Communities in Coastal Waters of Oman

K.A. Al-Hashmi[1], S.A.Piontkovski[1*], G. Bruss[1], W.Hamza[2], M.Al-Junaibi[2], Yu.Bryantseva[3] and E.Popova[4]

[1]Sultan Qaboos University, Sultanate of Oman.

[2]United Arab Emirates University, United Arab Emirates.

[3]M.G. Kholodny Institute of Botany, Ukraine.

[4]Institute of Biology of the Southern Seas, Russia.

Abstract

The monthly plankton sampling carried out in 2018-2019 has revealed over 190 phytoplankton species inhabiting coastal waters of the Sea of Oman. Diatoms were represented by 130 species, the highest diversity and total abundance of which were associated with the Northeast and Southwest Monsoon periods. Strong correlation was found between the abundance of diatoms, silicate and nitrogen concentrations. The dominance of diatoms was not consistent with previous reports which indicated the dominance of dinoflagellates in the coastal waters of the Sea Oman, in 2006-2017. An increase of diatoms stemmed from strong wind-induced mixing and high concentrations of silicates which level was about four fold less during the previous decade. Only few phytoplankton species formed huge algal blooms in studied regions. The dinoflagellate *Noctiluca scintillans* leads the list. The bloom development of this species lagged peaks of all the others. Copepods were the most abundant in the zooplankton fraction of plankton community. The abundance of 79 copepod species varied gradually over seasons. The main seasonal difference dealt with the number of carnivores, from genera *Labidocera, Sapphirina, Corycaeus*, and some others.

* Corresponding author: K.A. Al-Hashmi
Email ID: spiontkovski@gmail.com

INTRODUCTION

Seasonal variations of the structure and productivity of plankton communities is one of the most addressed issues in marine ecology. A number of overviews have synthesized current state of our understanding of seasonal cycles, on global and regional scales (Longhurst, 1998; Mackas et al., 2012; Nogueira et al., 2012; Piontkovski et al., 2019; Raymont, 1980; Smith et al., 1998). Nonetheless, many regions are lacking detailed studies (on the level of species) and the Gulf region is one of those.

The Sea of Oman (Gulf of Oman) is located in the northwest of the Arabian Sea and is connected to the Arabian Gulf by the Strait of Hormuz. A frontal zone formed during summer near the eastward cliff of Ras Al Hadd roughly separates the Sea of Oman from the entire Arabian Sea. Waters of the Sea of Oman are involved in a cyclonic circulation, which incorporates mesoscale cyclonic and anticyclonic eddies subjected to seasonal variations (L'Hegaret et al., 2015).

The surface waters are dominated by oceanic water that flows alongside the Iranian coast mixed with some cool advected water during winter (December to March) Northeast Monsoon (NEM). During summer (June-September), Southwest Monsoon (SWM), an upwelling persists along the south coast of Oman (Arabian Sea) and its effects can be observed in the Sea of Oman through the advection of cool water that reduces water temperatures during summer. Conditions off the northern coast of Oman are controlled by this advected water, strong heating during summer, the impact of an intense eddy field, the outflow of the Arabian Gulf and variable wind. (Quinn and Johnson, 1996; Harrison et al., 2019). Both, upwelling during SWM and convective mixing during NEM elevate nutrient level in the surface water of the Sea of Oman and consequently increase phytoplankton abundance (Al-Hashmi et al., 2015).

Coastal waters of Muscat possess a diverse assemblage of phytoplankton with a total of 278 taxa, reported. Dinoflagellates dominate the phytoplankton population most of the year and have higher number of species than diatoms (Al-Hashmi et al, 2015). Only occasionally, during NEM, diatoms overcome the dinoflagellate abundance as a result of higher silicate supply and cooler water (Al-Azri et al., 2010; Al-Hashmi et al., 2015). The dinoflagellate *Noctiluca scintillans* dominates phytoplankton during its bloom from July to September and from December to March, since late 1997.

Along with the *Noctiluca* blooms, the Sea of Oman experiences harmful algal blooms (Glibert, 2007; Richen et al., 2010), some of which are seasonal. Part of these blooms gets consumed by zooplankton while the other one, which could not be utilized by a trophic cascade, degrades and enriches sediment beds.

Another aspect of regional studies of the plankton seasonality is associated with the assessment of its role in seasonal variations of planktivorous fish stocks. Annual catches of small pelagic fishes by the Gulf Cooperation Council (GCC) countries are huge. In 2003-2016, sardines (represented mainly by the Indian oil sardine - *Sardinella longiceps* Valenciennes, *1847*) contributed 57% to artisanal landings of

small pelagic fishes by Oman, in the Sea of Oman (Fisheries Statistics Book, 2016).

In this paper, we analyzed seasonal changes of the phytoplankton and zooplankton fractions of epipelagic community, using simultaneous sampling complemented by CTD casts and remote sensing data. The goal was to elucidate the seasonality of the taxonomic structure, the size structure and the abundance of plankton over the studied regions. We also discuss trophic interactions between phytoplankton, zooplankton and small pelagic fishes, with a special reference to sardines.

MATERIALS AND METHODS

Remotely sensed data

Satellite-derived (4-km spatial resolution MODIS-Aqua) monthly Level-3 products for chlorophyll-*a* concentration were used, to assemble time series for the Muscat region, for the period of 2002-2019. These products are available from the National Aeronautics and Space Administration (NASA) Ocean Color Group (http://oceancolor.gsfc.nasa.gov). Monthly time series of chlorophyll-*a* and the wind stress were assembled using the GES-DISC Interactive Online Visualization and Analysis Infrastructure (GIOVANNI) software developed at NASA's Goddard Earth Sciences Data and Information Services Center.

In data analysis, the wind speed was characterized by its zonal and meridional components, which pointed at wind along the local parallel of latitude or longitude, respectively. Both characteristics have been transformed into the wind stress magnitude which is the amount of force impacting the surface. The wind stress depends upon wind velocity, drag coefficient and air density. It has units of Newtons per square meter. Data on the speed and the direction of the wind were also retrieved from (1) Aquarius Official Release Level 3 Wind Speed Standard Mapped Image 7-Day Running Mean Data V5.0, (2) the Live Access Server database which provides visualization and subsetting of multi-dimensional data worldwide (Hankin et al., 1998), and (3) Maps of wind speed at 10 meters based on Cross-Calibrated Multi-Platform Ocean Surface Wind Vector L3.5A Pentad First-Look Analyses (http://thredds.jpl.nasa.gov/thredds/dodsC/ncml_aggregation/OceanWinds/ccmp/aggregate__CCMP_MEASURES_ATLAS_L4_OW_L3_5A_5DAY_WIND_VECTORS_FLK.ncml).

Aerosol optical thickness at 869nm (AOT), photosynthetically available solar radiation (PAR) and air temperature (available as the MODIS-Aqua level 3 products at 4km spatial resolution) were retrieved from the GIOVANNI database in the form of weekly time series spatially averaged over regions (http://www.esrl.noaa.gov/psd/data/timeseries). Sea surface salinity JPL SMAP Level 3 CAP Sea Surface Salinity Standard Mapped Image Monthly V4.0 Validated Dataset was downloaded from the Live Access Server (https://podaac-tools.jpl.nasa.gov/las).

The data shown in Figure 3 were extracted from the satellite level 4 products as listed below; all data were accessed through the Ocean Products Portal of the Copernicus - Marine environment monitoring service (http://marine.copernicus.eu/services-

portfolio/access-to-products/) where extensive descriptions of the datasets can be found. Wind:

CERSAT -WIND_GLO_WIND_L4_REP_OBSERVATIONS_012_006;

Sea surface temperature:

OSTIA - SST_GLO_SST_L4_NRT_OBSERVATIONS_010_00;

Geostrophic flow:

DUACS - SEALEVEL_GLO_PHY_L4_NRT_OBSERVATIONS_008_046

Direct sampling

Temperature, salinity, oxygen and depth were measured with an Idronaut-Ocean Seven 316 CTD probe fitted with an additional sensor for chlorophyll-*a* fluorescence. Subsurface water samples that were representative of the mixed layer were collected with Niskin bottles for the analyses of nitrate + nitrite, ammonium, phosphate and silicate. After collection, water samples were frozen and analyzed later, for nutrients using a 5-channel SKALAR FlowAccess auto-analyzer according to the procedures described by the manufacturer of the analyzer (Skalar Analytical 1996).

CTD casts and plankton sampling were conducted off the Muscat coast at 23º35'N and 58º 43'E (maximum depth, 100 m) and in the Sohar region, in which the depth was about 20m (Figure 1).

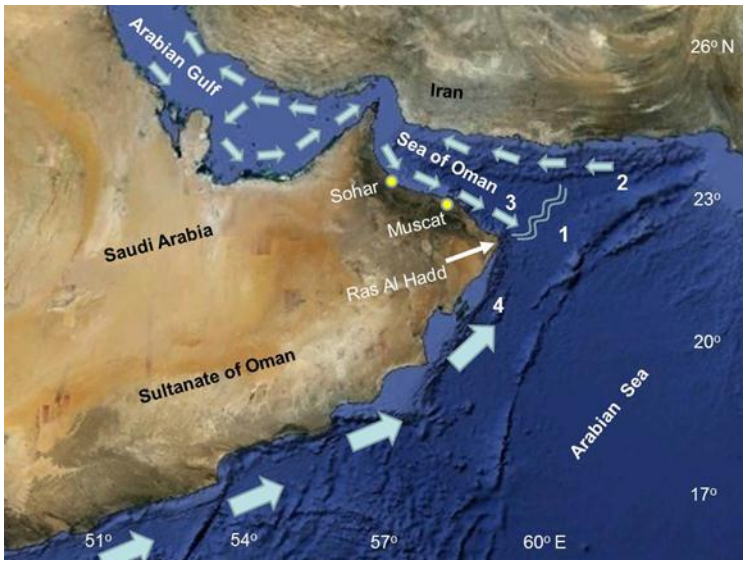

Figure 1. Location of sampling sites (in yellow) and a scheme of regional circulation. 1: the Ras Al Hadd frontal zone formed by the confluence of the East Oman Current (3) and Oman Coastal Current (4). Arrows (2-4) indicate direction of currents during the Southwest Monsoon. 2: inflow of the Indian Ocean Water mass. The East Oman Current (3) also shows the outflow of the Persian Gulf Water mass.

For phytoplankton species identification and cell counts, water samples (250 ml) were collected and preserved with 2% Lugol's iodine solution. Species identification was done under light microscope "Carl Zeiss" at 10x, 20x and 40x magnification. A Sedgwick camera (1ml) was used for cell counting. Identification was done at the species or genus level, although some taxa could not be identified and were ranked as the category (such as "Small flagellates"). Species identification was based on appropriate references (Al-Hashmi, 2017; Sournia, 1986; Round, 1990; Tomas, 1997; Al-Yamani, Saburova, 2019 a; Al-Yamani, Saburova, 2019 b).

Zooplankton samples were collected twice a month, from June 2018 through May 2019. The Muscat waters were the most sampled, in terms of the gaps revealed in primary data. Therefore, our data analysis was focused on the monthly time series resembling variability in this region. The zooplankton were sampled vertically, using the net with the frame diameter of 60 cm and the mesh size of 200 micrometers. Samples were preserved in 5 % neutral formalin and processed later in the lab. A binocular microscope (model SZ-X7) was used to identify, enumerate and measure specimens.

Data on monthly landings for sardines were retrieved from the annual reports published by the Omani Ministry of Agriculture and Fisheries (Fishery Statistics Book, 2016, 2018).

Statistical analysis

The Cluster Analysis in "Statistica v.9" was employed, to elucidate statistical links between the plankton community and environmental parameters arranged in the form of monthly time series covering the sampled time range. Missing data were case wise deleted. The weighted pair-group averaging and the Euclidean distance metric were used, to construct the dendrogram. The Principle Component Analysis (PCA) (Warwick and Clarke, 1991) was applied, to correlate the log-transformed characteristics of phytoplankton community with environmental variables.

Low-pass filtered (48h) wind from the CERSAT data was averaged over 75km around the sampling station offshore of Muscat. Diurnal geostrophic flow from the DUACS data was averaged over 3 nearshore pixels around the sampling station offshore Muscat.

RESULTS

Winds and geostrophic flow

Annually averaged patterns of a wind rose in the Muscat region, pointed out the prevailing north-east direction (Figure 2), which corresponds to the direction of winter monsoon winds over the Arabian Sea (L'Hegaret et al., 2015). The spatial pattern of wind directions showed some regional differences.

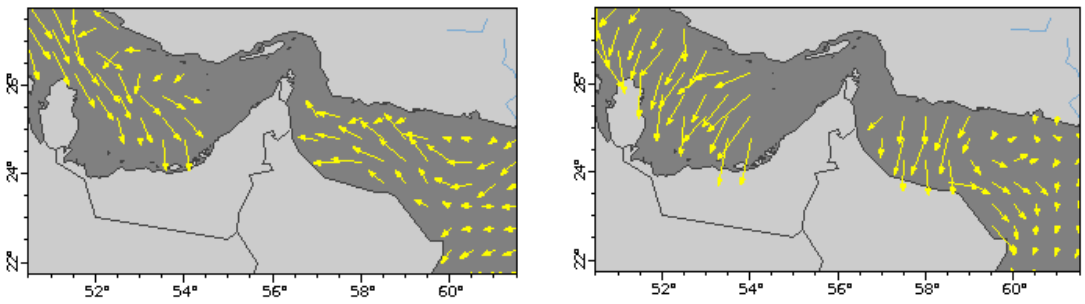

Figure 2. Upper panel: distribution of the wind direction (%) over regions. Annually averaged data on daily wind direction covered the period from May-2003 to February-2018 (7am-7pm local time; https://www.windfinder.com). Mid and Low panel: wind vectors at sea surface, in January (mid panel) and October-2018 (low panel). Y-component: 5 ms^{-1}(upper panel) and 2 ms^{-1}. NOAA/NCDC blended daily 0.25º sea surface winds. Data courtesy of NOAA NCEI.

Seasonal alterations were pronounced throughout the annual cycle of 2018-2019. Pictures are based on the NOAA/NCDC blended daily global 0.25º remotely sensed data (10m altitude). As far as the wind speed is concerned, annually averaged values based on meteorological stations along the coast did not show much difference; 92% of seasonal fluctuations span the range between 5 and 4 m s^{-1}. However, gusts of the northeasterly winds attain the speed of ~15 m s^{-1}.

The monthly panels for wind offshore of Muscat (Figure 3) show stronger wind during the winter months (December-March) with high variability mostly along the north-west/south-east axis. Despite higher wind velocities in winter, monthly averages remain low due to high directional scatter. Weaker winds during the summer monsoon (July-September) show less scatter with monthly residuals towards north-west. Wind conditions during the sampling period (July 2018-June 2019) mostly follow the patterns of previous years while frequent events of strong wind are apparent in early 2019. Figure 2 illustrates the spatial variability of the regional wind.

The monthly panels for geostrophic surface flow in Figure 3 reveal seasonal changes with lower variation during summer (April-September) and higher inter-annual variability during winter. Distinct residual flow around Muscat (blue crosses) only appears after the SWM (October-November) predominantly directed towards south-east. The flow during the sampling period deviates from conditions of previous years during July-August 2018 and May 2019 when unusually strong flow is directed towards north-west.

Thermo-haline characteristics of waters

The central panels of Figure 3 illustrate the multi-modal pattern of the annual sea surface temperature (SST) around Muscat. Four characteristic conditions can be distinguished: a summer high in June-July before the SWM, a summer low during the

SWM in August, a second (lower) summer high after the SWM in early October and a winter low in February. The highest inter annual variation of the local SST appears during the period of the SWM. This general pattern appears along the entire northern Omani shelf. Spatial variations are mainly related to a general increase of summer temperatures towards the north-west.

Figure 3 compares conditions during the 12 month sampling period (July 2018-June 2019) to the 9 preceding years and their mean. The SST recorded during the sampling period remains distinctly below the 9 year average during August-October 2018 and March and May 2019. In July-August 2018 and May 2019 unusually strong flow compared to previous years is directed towards northwest. In February-March 2019 weak flow coincides with strong alternating wind.

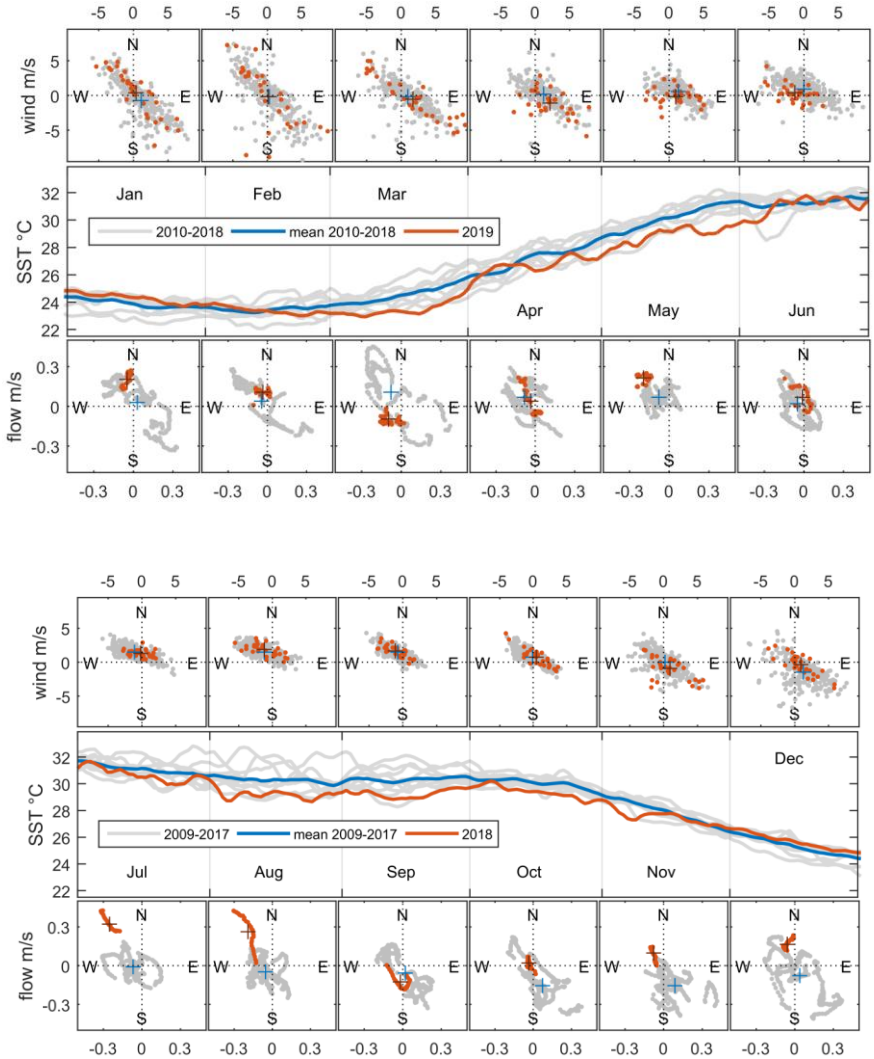

Figure 3. Wind, SST and geostrophic surface flow for the region around Muscat. The points in the monthly panels of the vector data (wind and flow) represent the tip of diurnal "going-to" vectors. Dark-brown and blue crosses indicate monthly averages of the sampling period and the preceding 9 years respectively.

The annual distribution of temperature shows semi-annual mode of variability, with two warming and two cooling phases (Figure 4). The major warming occurs during May through July, with SST exceeding 32℃ in July in both sampling sites. The minor warming occurred during October with a peak SST around 30℃ in Muscat and 31℃ in Sohar region. The minor warming phase was less intense compared to the major warming phase. Due to intense heating of the surface, the mixed layer and the thermocline remained shallow during May-July but deepened during secondary warming phase. The 26℃ isotherm, taken as the top of the thermocline, was around 12 m depth during primary warming phase, while it penetrated down to 18 m depth during secondary warming, in October. The cooling phases occurred during December-April and July -September.

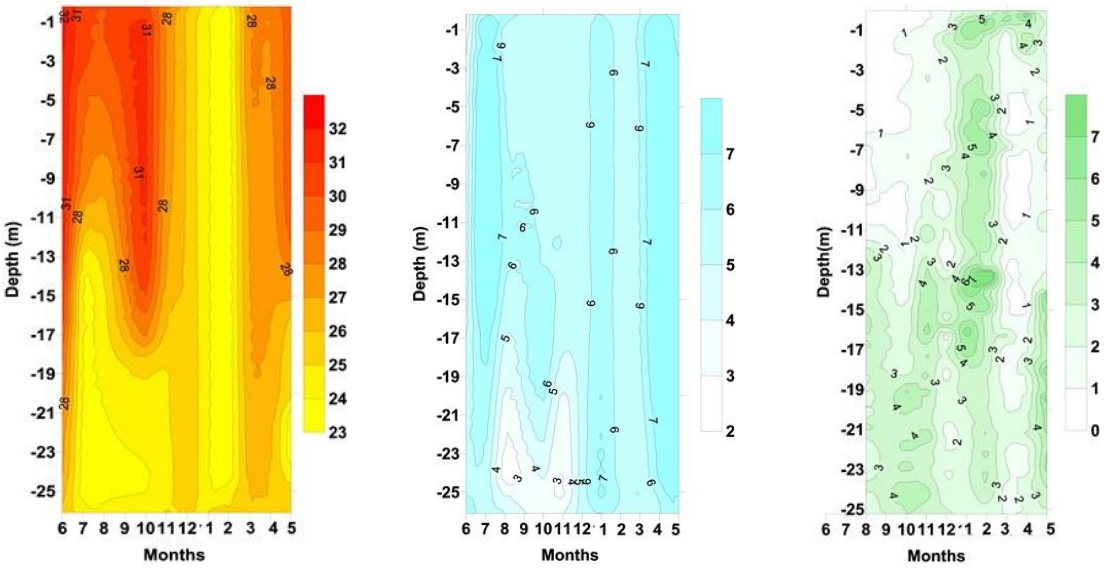

Figure 4. Seasonal variations of the vertical distribution of temperature (left panel), dissolved oxygen (middle panel) and chlorophyll-*a* (right panel) in coastal waters of Sohar, in 2018-2019.

The major cooling was very intense compared to the secondary cooling phase. The SST dropped to < 23℃ during the primary cooling phase and the cool waters penetrated to the bottom. The thermocline was completely eroded during the winter cooling phase with cool waters extending up to bottom while during July-September it raised towards surface indicating upwelling event. The vertical displacement of the isotherms was considerable during the phase shifts (warming/cooling).

The dissolved oxygen (DO) distribution (Figure 4) showed an annual cycle largely similar to that of the temperature in both sampling sites. The upper 15 m showed high level of oxygen concentrations (6-7 mg L^{-1}) during the sampling periods, except in June and late September till early December, when the concentration ranged between 4 and 5 mg L^{-1}. The low DO phases occurred during August-November when the DO

concentration dropped to about 3 mg L^{-1} below 20 m depth. Mixing was more pronounced during the cold phases (January-February) characterizing the high oxygen phase.

Chlorophyll-a

Chlorophyll-*a* showed a similar seasonal variation at both sampling sites. In the mixed layer in Sohar, chlorophyll-*a* concentration remained below 1 µgl L^{-1} from August until November while in Muscat, during the same period, values varied between 1 and 3 µgl L^{-1}. Maximum surface chlorophyll-*a* (5 µgl L^{-1}) was attained on February and August in coastal waters of Sohar and Muscat. Chlorophyll maximum depth was found to be between 10 and 15 m in Sohar and between 10 and 25 m in Muscat. In Muscat, chlorophyll-*a* reached maxima in September when values ranged from 10-20 µgl L^{-1}, whereas chlorophyll maximum in Sohar was about 7 µgl L^{-1}, in February.

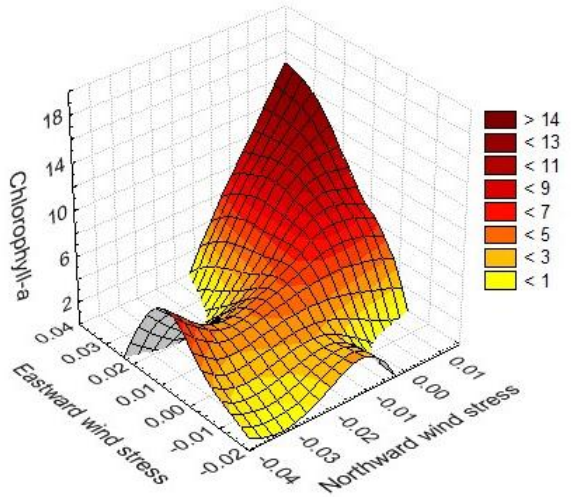

Figure 5. Three-dimensional scheme of the relationship between chlorophyll-*a*, zonal and meridional components of the wind stress (N m^{-2}). The plot was smoothed by the Distance Weighted Least Squares Method. Color bar stands for the chlorophyll-*a* concentration (mg m^{-3}).

Retrospective analysis of 17 year monthly remotely sensed chlorophyll-a concentration in the Muscat region (in the one degree square box which framed our sampling site) showed that 74% of the peaks observed in 2002-2019, matched the time of the NEM. In order to elucidate the relationship between remotely sensed chlorophyll-*a*, zonal and meridional components of the wind speed, a three-dimensional diagram was employed (Figure 5). Positive and negative values of the wind speed components depend on the direction. The zonal wind is positive if it blows from West towards East. The meridional wind is positive if it blows from South

towards North. The wind-induced mixing of the upper layer is rather associated with the wind stress than the wind speed. In this regard, the plot we used, implied maximal concentrations of chlorophyll-*a* to be associated with peaks of zonal and meridional wind stress.

Phytoplankton abundance

The processing of phytoplankton samples revealed 249 species in Muscat regions and 192 species in Sohar regions. The monthly sampling implied the presence of a similar pattern in the distribution of species over classes throughout the year (Figure 6). Diatoms and dinoflagellates represented more than 50 % and 30 % of the total species number in both regions respectively. Other 12 groups represented less than 20% with very low abundance contribution, therefore are neglected.

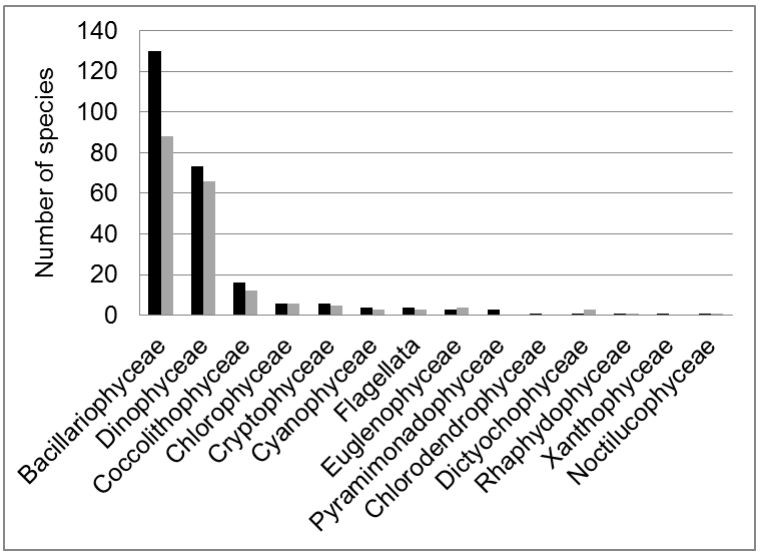

Figure 6. Distribution of the number of phytoplankton species over classes. Black and grey bars stand for the Muscat and Sohar region, respectively.

On the level of taxonomic classes, diatoms (*Bacillariophyceae*, 130 species) dominated over all the others, in the upper 20m layer. Maximal concentrations of phytoplankton were observed at surface and in the subsurface chlorophyll maximum (at about 20m, in waters of Muscat).

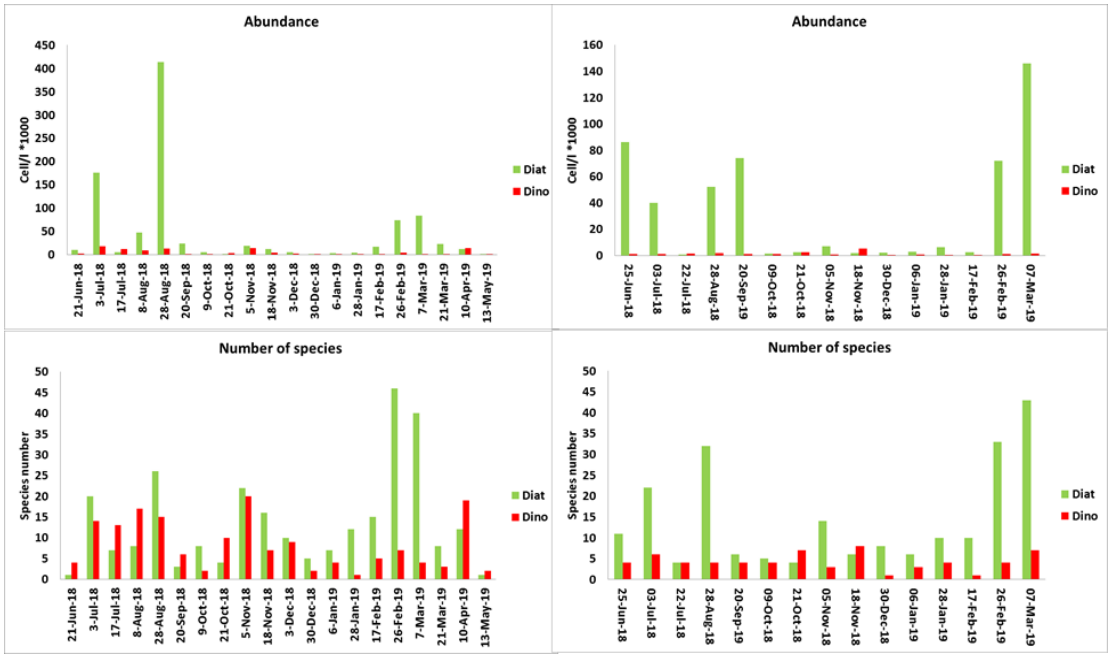

Figure 7. Monthly abundance and number of species of phytoplankton in coastal waters of Muscat (surface layer, left panel; 20m depth, right panel). Diat: diatoms, Dino: dinoflagellates.

The seasonal dynamic of the abundance at surface showed that diatoms of the Muscat region have exhibited a bimodal pattern, in which the major peak was observed in August, followed by a minor peak in February through March, while the peaks were reversed at 20 m.

The diatom abundance in coastal waters of Sohar showed higher peak in February both at surface and 20 m depth with unusually high abundance in May (Figure 8). Also, high abundance was indicated by high satellite chlorophyll-*a*, during May.

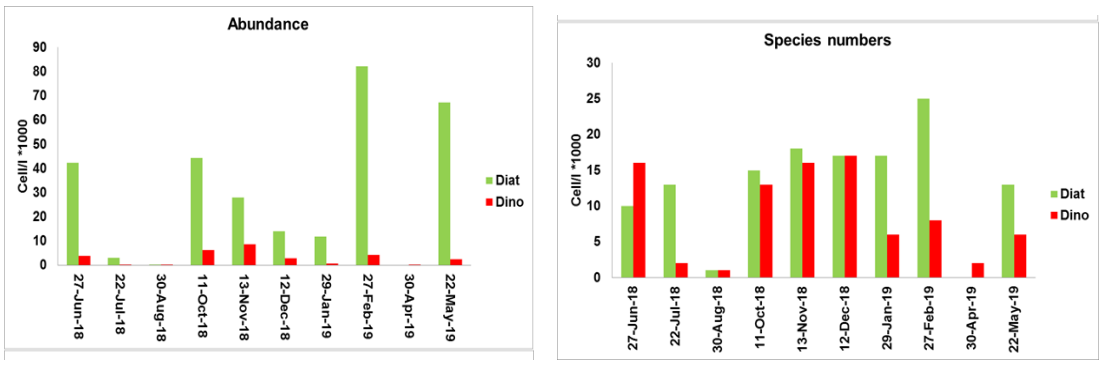

Figure 8. Monthly abundance and number of species of phytoplankton in coastal waters of Sohar (surface layer).

The diatom species, which formed maximal concentrations were different over regions. *Dactyliosolen fragilissimus* (centric diatoms) attained the highest concentrations at surface in Muscat waters during August 2018, while *Chaetoceros*

socialis (centric diatoms) dominated the 20 m depth in February 2019. In Sohar, *C. socialis* exhibited the highest concentrations at surface (Table 1). The genus *Chaetoceros* was the dominate genus in Sohar and Muscat during winter (Jan- April) at surface and 20 m depth while summer population composed of mixed benthic and centric diatoms (Table 1).

Table. 1. Episodes of maximal concentrations of phytoplankton species in coastal waters of Muscat and Sohar.

Date	Diatom species Muscat region	Species abundance, cell m^{-3}	Total diatom abundance, cell m^{-3}	%
25 Jun 2018	*Haslea balearica*	83812	86624	97
3 Jul 2018	*Skeletonema grevillei*	10120	40112	
	Bacteriastrum delicatulum	9660		
22 Jul 2018	*Cyclotella stylorum*	192	672	29
	Pleurosigma diversestriatum	192		29
28 Aug 2018	*Dactyliosolen fragilissimus*	218724	412893	51
	Hemiaulus hauckii	5341		10
20 Sep 2018	*Haslea balearica*	73320	74256	99
9 Oct 2018	*Haslea balearica*	500	1600	31
21 Oct 2018	*Thalassiosira minima*	2016	2576	78
5 Nov 2018	*Thalassiosira minima*	1568	7168	22
18 Nov 2011	*Nitzschia bicapitata*	864	1728	50
30 Dec 2018	*Proboscia alata*	1044	2088	50
6 Jan 2019	*Chaetoceros socialis*	1200	2760	43
28 Jan 2019	*Chaetoceros pseudocurvisetus*	1456	6384	23
17 Feb 2019	*Chaetoceros costatus*	840	2520	33
26 Feb 2019	*Chaetoceros socialis*	28800	71880	40
	Bacteriastrum delicatulum	8640		12
7 Mar 2019	*Chaetoceros socialis*	23760	146160	16
	Chaetoceros costatus	23520		16
	Chaetoceros pseudocurvisetus	14640		10

Date	Diatoms species Sohar region	Species abundance, cell m^{-3}	Total diatom abundance, cell m^{-3}	%
27 Jun 2018	*Guinardia striata*	26404	42228	63
22 Jul 2018	*Bacillariophyceae sp.*	608	3040	20
30 Aug 2018	*Pseudo-nitzschia delicatissima*	5984	10784	56
11 Oct 2018	*Guinardia striata*	19980	87972	23
13 Nov 2018	*Leptocylindrus minimus*	10080	122800	8
	Thalassiosira decipiens	16800		14
	Pseudo-nitzschia pungens	11040		9
	Cerataulina pelagica	9600		8
	Chaetoceros costatus	7800		6
12 Dec 2018	*Skeletonema grevillei*	21384	35964	60
29 Jan 2019	*Chaetoceros pseudocurvisetus*	16240	111868	15
	Eucampia zodiacus	12760		11
	Lauderia annulata	23316		21
27 Feb 2019	*Chaetoceros socialis*	61448	182704	34
	Skeletonema grevillei	19728		11
	Chaetoceros pseudocurvisetus	14400		8
22 May 2019	*Bacteriastrum hyalinum*	31968	67284	48
	Chaetoceros tortissimus	18792		30

Dinoflagellates (*Dinophyceae*, 88 species) were inferior in abundance compared to diatoms in all sampling periods and only overcome the diatoms population in July and October in Muscat and in July in Sohar. This period characterized the lowest phytoplankton abundance (not taking into account the *Noctiluca scintillans* bloom). Dinoflagellates were better represented during July, November and April in coastal waters of Muscat. *Scrippsiella irregularis Akashiwo sanguinea* and *Gymnodinium simplex* were the most important taxa during that periods. However, dinoflagellates were more abundant in October and in November in Sohar waters, when *Heterocapsa rotundata, Heterocapsa pygmaea, Prorocentrum balticum and Gymnodinium simplex* were the most common taxa .

A periodic (oscillating) pattern of the number of species was observed in the Muscat region (Figure 7). For instance, diatoms (the dominant group) exhibited multiple peaks throughout the year of sampling. The major peak of diatoms species number (46 species) was observed during winter (Feb-March) and the minor peak (26 species) was in August. The seasonal pattern in the Sohar region was much more smoothed and showed a long-term increase in the number of diatom species (15-25 species) throughout the NEM, from December through February (Figure 8).

Dinoflagellates, in coastal waters of Muscat, achieved their highest number of species in November and April (19 and 20 species) while in Sohar, the highest species number with 16, 16, and 19 species, were recorded in June, November and December respectively.

Noctiluca scintillans formed huge peaks of abundance (up to $3*10^6$ cells per cubic meter) during the end of fall inter-monsoon and onset of the Northeast Monsoon season (Figure 9).

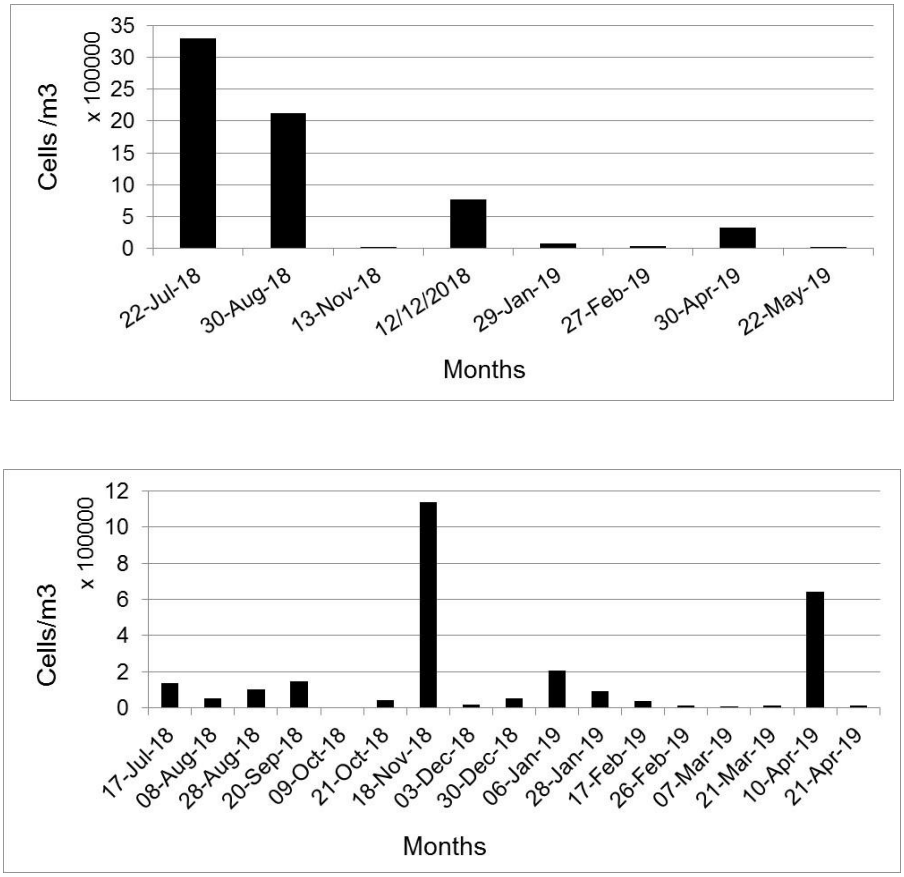

Figure 9. Concentrations of *Noctiluca scintillans* (cells m^{-3}) in coastal waters of Muscat (low panel) and Sohar (upper panel).

These blooms have had the life span from two to four weeks. The diameter of cells varied from 0.5 to 0.9 mm. The magnitude of summer bloom in Sohar coastal waters markedly (24 times) exceeded the one observed in the Muscat region (Figure 9 and Table 2). Apparently, the seasonal pattern of this (periodically dominant) species experiences marked changes of the onset, magnitude and life time of winter and summer blooms, over years.

The seasonal dynamics of diatoms was consistent with the seasonal pattern of nutrients (Figure 10). The concentrations of nitrate (NO_3) and silicate (SO_4) in both sampled regions have exhibited seasonal peaks in July and August, followed by a broad-band peak in January through March.

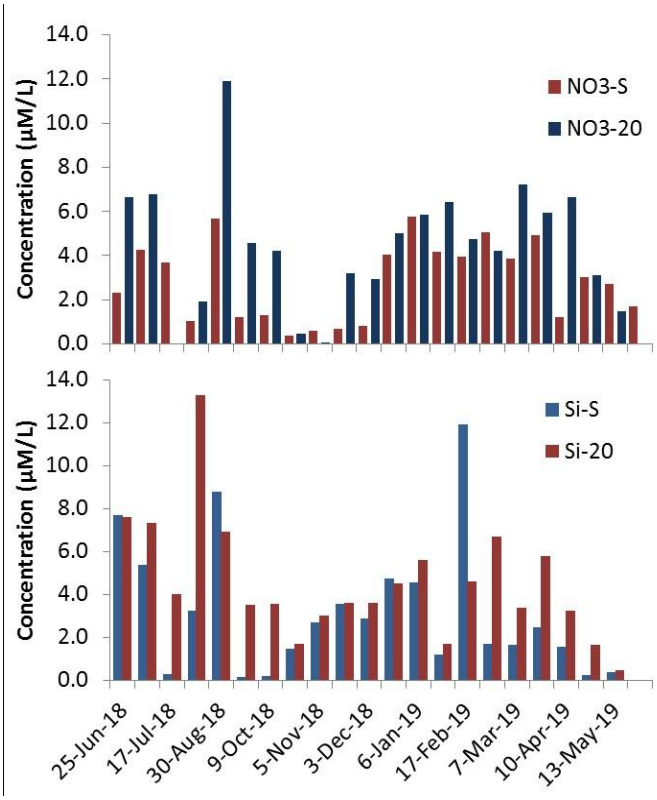

Figure 10. Seasonal changes of the concentration of nitrate (NO_3/µL) and silicate (SiO_4/µL) at the surface (S) and 20 m depth in coastal waters of Muscat.

Generally, the concentrations of nutrients (NO_3, SiO_4) in the 20 m depth were higher than the surface water. Major peaks of both nutrients (8-12 µL) were recorded during August-September and January-March. The lowest values (below 2 µL) were observed during October to November and from May to June. The concentrations remained close to 4 µL during the rest of the year.

In analyzing phytoplankton, one should take into account the role of the dinoflagellate *Noctiluca scintillans,* which is usually sampled by a zooplankton net. Our zooplankton sampling showed that this species formed huge peaks of abundance (up

to $3*10^6$ cells per cubic meter) by the end of fall inter-monsoon and onset of the NEM season. The *Noctiluca* blooms have had the life span from two to four weeks. The diameter of cells varied from 0.5 to 0.9 mm. The magnitude of summer bloom in Sohar coastal waters markedly (24 times) exceeded the one observed in the Muscat region. Our data on current and previous sampling enabled some features of seasonal and interannual variability of *Noctiluca* blooms to be elucidated (Table 2).

Table 2. Seasonal pattern of the abundance peaks, of some abundant phytoplankton species (Muscat region).

Class	Species/months	1	2	3	4	5	6	7	8	9	10	11	12
Bacillariophyceae	*Pseudo-nitzschia delicatissima*							■					
Bacillariophyceae	*Leptocylindrus danicus*								■				
Bacillariophyceae	*Thalassiosira minima*								■				
Bacillariophyceae	*Haslea balearica*									■			
Bacillariophyceae	*Dactyliosolen fragilissimus*								■				
Bacillariophyceae	*Pseudo-nitzschia multistriata*		■										
Bacillariophyceae	*Pseudo-nitzschia delicatissima*							■					
Bacillariophyceae	*Chaetoceros compressus*							■					
Bacillariophyceae	*Chaetoceros socialis*			■									
Bacillariophyceae	*Skeletonema grevillei*							■					
Bacillariophyceae	*Leptocylindrus minimus*							■					
Bacillariophyceae	*Bacteriastrum delicatulum*		■										
Bacillariophyceae	*Chaetoceros affinis*		■										
Bacillariophyceae	*Chaetoceros curvisetus*							■					
Bacillariophyceae	*Pseudo-nitzschia seriata*								■				
Bacillariophyceae	*Thalassionema nitzschioides*							■					
Dinophyceae	*Gymnodinium simplex*							■					
Cyanophyceae	*Trichodesmium errythraeum*							■					
Dinophyceae	*Noctiluca scintillans*				■							■	

Apparently, the seasonal pattern of this (periodically dominant) species experiences marked changes of the onset, magnitude and life time of winter and summer blooms, over years. The comparison of remotely sensed chlorophyll-a in the Sea of Oman with a direct sampling of plankton, elucidated a good match.

Zooplankton

Zooplankton were represented by 79 species of copepods (which was the most abundant group of zooplankton), followed by *Appendicularia* (family *Oikopleuridae*), *Thaliacea* (*Doliolida*), and *Chaetognatha* (*Sagittoidea*). The body length of zooplankton organisms varied from 0.3 to 200 mm. The largest individuals were represented by *Chaetognatha*. Among copepods, the most abundant species were *Canthocalanus pauper, Acrocalanus longicornis, Paracalanus indicus, Clausocalanus furcatus, Calocalanus plumulosus, Centropages furcatus, Oncaea clevei, Subeucalanus pileatus var. "right*" and some others (Table 3).

Table 3. Copepod species, their size range, abundance and feeding types (the Sea of Oman). Acronyms: H-herbivore species; C-carnivore species; O-omnivore species. Abundance min: minimal abundance. Abundance max: maximal abundance.

Copepod species	Size range, mm	Abundance min (ind. m^{-3})	Abundance max (ind. m^{-3})	Type of feeding
Acrocalanus gracilis	0.8-1.5	7	5,257	H
Acrocalanus longicornis	0.6-1.5	8	7,885	H
Acartia amboinensis	0.7-1.5	7	9,856	O
Bestiolina arabica	0.80	22	44	H
Calocalanus plumulosus	0.7-1.2	3	986	H
Canthocalanus pauper	1.0-1.7	3	1,314	H
Centropages furcatus	0.8-1.5	7	1,643	H
Centropages orsinii	0.9-1.8	5	66	O
Clausocalanus farrani	1.1-1.4	7	905	
Clausocalanus furcatus	1.1-1.4	42	5,914	
Clausocalanus spp.	0.6-1.0	4	2,628	
Clytemnestra spp.	0.8-1.1	3	66	
Copilia mirabilis	1.0-4.7	3	657	C
Corycaeus andrewsi	0.9-1.0	7	329	C
Corycaeus lubbocki	0.9-1.0	7	164	C
Corycaeus subtilis	0.80	11	30	C
Corycaeus speciosus	1.7-2.1	5	131	C
Corycaeus agilis	1.0-1.1	7	3,614	C
Corycaeus catus	0.90	7	12	C
Corycaeus crassiusculus	1.6-1.8	10	31	C
Corycaeus erythraeus	1.0-1.1	7	657	C
Corycaeus dahli	1.00	10	12	C
Corycaeus pacificus	1.1-1.2	3	657	C
Corycaeus spp.	0.7-1.6	6	8,542	
Euchaeta indica	2.5-2.7	5	394	C
Euchaeta spp.	0.8-3.0	4	66	
Euchaeta rimana	3.3-3.7	3	50	C
Euconchoecia aff.aculeata elongata	0.5-1.6	10	657	

Euterpina acutifrons	0.6-0.8	22	110	O
Farranula gibbula	0.80	6	6	C
Farranula spp.	0.80	21	30	
Labidocera acuta	2.25-3.5	5	427	C
Labidocera bengalensis	1.7-3.0	11	197	C
Labidocera spp.	1.1-1.6	10	41	C
Lucicutia cf. flavicornis	1.40	5	6	C
Lucicutia gaussae	1.20	10	12	C
Macrosetella gracilis	1.00	14	14	
Nannocalanus minor	1.4-2.2	5	329	H
Oithona attenuata	0.75	10	22	O
Oithona brevicornis	0.6-0.7	22	77	O
Oithona fallax	0.8-0.9	6	110	O
Oithona nana	0.6-0.7	7	60	O
Oithona plumifera	1.2-1.3	15	657	O
Oithona spp.	0.2-1.1	14	986	
Oncaea venusta	0.9-1.4	6	1,314	C
Oncaea clevei	0.7-0.8	17	7,885	C
Paracalanus aculeatus	0.9-1.4	3	2,628	H
Paracalanus aculeatus minor	0.8-1.0	3	6,571	H
Paracalanus denudatus var.	0.8-1.0	57	6,571	H
Paracalanus indicus	0.8-1.0	25	6,899	H
Paracalanus spp.	0.7-0.9	8	6,571	H
Paracalanus tropicus	0.7-0.8	12	329	H
Paraeuchaeta concinna	2.5-3.0	5	66	
Parvocalanus elegans	0.5-0.6	29	121	
Pleuromamma spp.	0.8-1.6	5	12	O
Pseudodiaptomus arabicus	1.1-1.5	8	31	
Pseudodiaptomus serricaudatus	1.0-1.5	7	329	
Sapphirina nigromaculata	1.6-2.0	5	197	C
Sapphirina darwini	2.20	66	66	C
Sapphirina spp.	0.7-1.8	5	110	C
Scolecitrichopsis ctenopus	1.60	6	11	H
Scolecithricella longispinosa	1.10	5	22	
Scolecithricella paramarginata	1.1-1.2	5	30	
Subeucalanus crassus	1.2-2.8	5	66	H
Subeucalanus pileatus var. "right"	1.1-2.3	3	1,095	H
Subeucalanus pileatus	1.1-2.3	4	329	H
Subeucalanus mucronatus	2.1-2.7	4	20	H
Subeucalanus subtenuis	1.1-2.2	4	1,095	H
Subeucalanus subcrassus	1.1-2.6	5	657	H
Temora discaudata	0.9-2.0	7	657	O
Temora turbinata	0.5-1.3	11	1,582	O
Triconia conifera	1.10	15	61	O

No changes were observed in the number of copepod species over seasons. We analyzed published data on feeding strategies of the species listed in the table and assigned appropriate acronyms. Feeding types were retrieved from papers and the databases resembling these preferences (Chen et al., 2018; Turner, 1984, 2004; https://copepodes.obs-banyuls.fr/fichesp.php?sp=1823 and etc.). The majority of abundant species observed in Omani coastal waters were herbivores, although the feeding strategy of copepods is believed to be fairly flexible (Kleppel, 1993).

The observed tendency of species occurrence matched the one reported for subtropical and tropical waters of the world's ocean, in which each copepod species contributes just few percent to the total copepod abundance. Seasonal patterns of copepod species abundance were quite variable; some demonstrated one peak, in August, as exemplified by *Acrocalanus longicornis*. The other species (*Clausocalanus furcatus*, *Oncaea clevei* and some others) exhibited two peaks, in August and November (Figure 11). The main seasonal difference of the trophic structure dealt with the number of carnivores, from genera *Labidocera*, *Sapphirina*, *Corycaeus*, and some others.

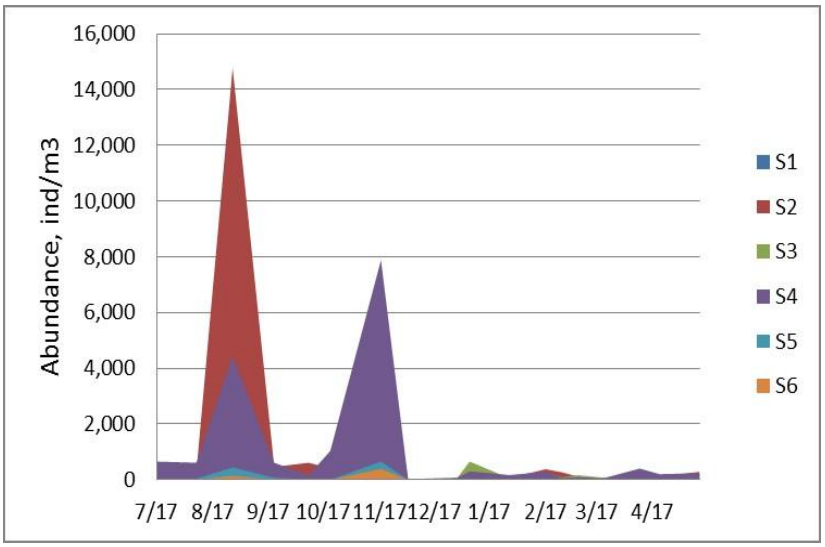

Figure 11. Seasonal changes of the copepod species abundance in waters of Muscat. S1*: Calocalanus plumulosus, females*, S2: *Acrocalanus longicornis*, females, S3: *Clausocalanus furcatus*, females, S4: *Oncaea clevei*, females, S5: *Copilia mirabilis*, females, S6: *Euchaeta indica*, females.

Peak magnitudes varied gradually over species- from 51,000 individuals per cubic meter to 15,000 individuals per cubic meter. Along with copepods, arrow worms (*Sagitta spp.*) and cladoceran species (*Penilia avirostris* and *Pseudevadne tergestina)* attained maximal concentrations of about 3,000 ind. m^{-3}, 20,000 ind. m^{-3} and 147, 000 ind. m^{-3}, in August, respectively. Arrow worms are predators, which have had the size from 1 to 20mm, in our samples. Cladoceran species (fine-filter feeders) varied in size

from 0.5 to 1.2 mm. No statistical difference was found between the copepod total abundance, in Muscat and Sohar regions. Multiple statistical coupling between physical, chemical and biological characteristics in the Muscat region was analyzed by means of the Cluster Analysis (Figure 12).

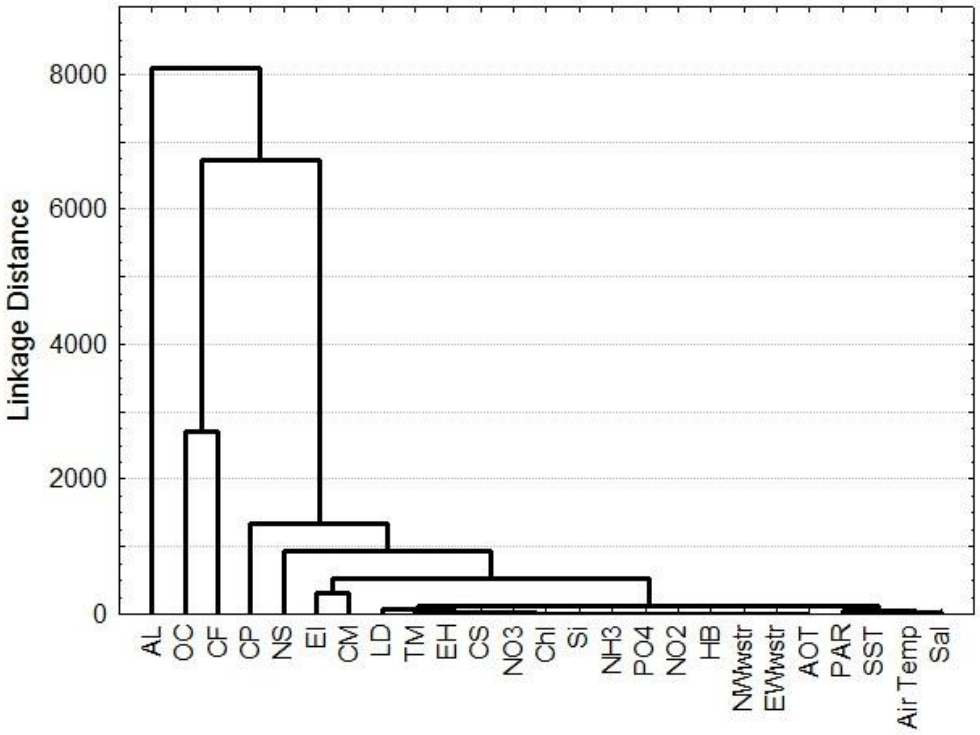

Figure 12. Dendrogram of Euclidean distances between variables and clusters (the Muscat region). Acronyms: AL-*Acrocalanus longicornis*, OC-*Oncaea clevei*, CF-*Clausocalanus furcatus*, CP-*Clausocalanus plumulosus*, NS-*Noctiluca scintillans*, EI-*Euchaeta indica*, CM-*Copilia mirabilis*, LD-*Leptocylindricus danicus*, TM-*Thalassiosira minima*, EH-*Emilianya huxsleyi*, CS-*Chaetoceros socialis*, NO3-nitrates, Chl-chlorophyll-*a*, Si-silicates, NH3-ammonium, PO4-phosphates, NO2-nitrites, HB-*Halsea balearica*, NWwstr-Northward surface wind stress, EWwstr-Easward surface wind stress, AOT-Aerosol optical thickness, PAR-Photosynthetically available solar radiation, SST-Sea surface temperature, Air Temp-Air temperature at sea surface, and Sal-Salinity at sea surface.

In monthly variations, *Noctiluca* exhibited high clusterization with small-sized herbivore copepods (*Acrocalanus longicornis, Clausocalanus furcatus, and Clausocalanus plumulosus*), although *Oncaea clevei* (the carnivore species) was in this cluster as well. The strength of the cluster incorporating these 4 species markedly exceeded all the others.

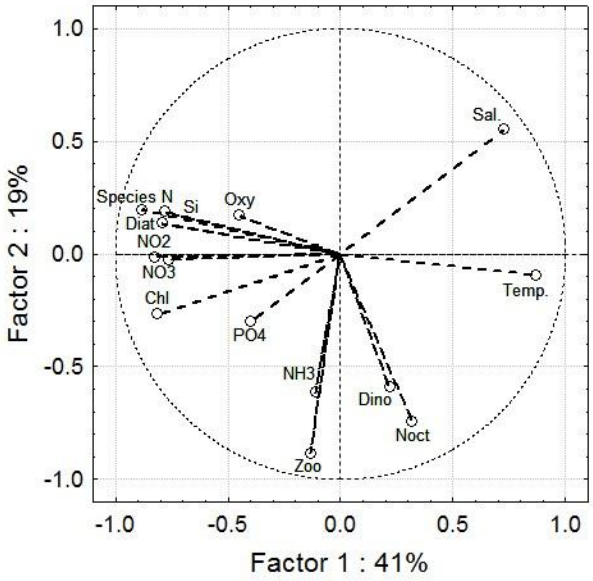

Figure 13. PCA analysis showing the grouping diatoms and dinoflagellates, and their relationship to the environmental parameters (20m depth). Temp: temperature; Sal: salinity; Oxy: dissolved oxygen concentration; Chl: chl-*a* concentration; NH3: ammonium; NO2: nitrite; PO4: phosphate; NO3: nitrate; Si: silicate concentration; Diat: diatom abundance; Dino: dinoflagellate abundance; Zoo: total abundance of zooplankton; Noct: abundance of *Noctiluca*; Species N: total number of phytoplankton species.

All the data collected in Muscat coastal waters at 20m depth were subjected to the Principal Component Analysis (Figure 13), in which the first two Factors explained 60% of the total variability in the system of selected variables. Diatoms dominated by a statistical load to the Factor 1. Highest clusterization, with negative signs, was observed between diatoms, silicates, nitrites, nitrates, chlorophyll-*a* and the total number of phytoplankton species. Temperature and salinity contributed markedly as well, but with positive signs. The group of listed variables has dominated by their contribution to the Factor 1 loading. The Factor 2 was contributed mainly by *Noctiluca* and the total zooplankton abundance. Clusterization in Factor 2 reflected the competition of *Noctiluca* and all zooplankton organisms for the food source (phytoplankton cells).

DISCUSSION

Diatoms were the dominant phytoplankton group in the Sea of Oman during the sampling period. The abundance of diatoms was closely related to the availability of nutrients. Therefore, strong correlation was found between the abundance of diatoms and silicate and nitrogen concentrations (Figure 13). Diatoms are normally very abundant during periods of high new production (i.e., production based on

accumulated nitrate), i.e during upwelling seasons when nutrients and light are optimal as diatom higher growth rate enables them to outcompete dinoflagellates ((Brand and Guillard, 1981; Reynolds, 2006). Diatoms were also found to be the main contributor to chlorophyll concentrations and species number (Figure 13) especially during the monsoon seasons.

There were more diatoms compared to the other plankton types when there was no stratification namely during SWM and NEM, when the thermocline was completely eroded. On the other hand, dinoflagellates were available during the time of low turbulence, higher temperature stratification and when nutrients were mostly depleted. Diatoms have a larger range of the wind-induced mixing at which they dominate unlike dinoflagellates that dominate more at lower wind impact. There was higher diatoms abundance during SWM than NEM, but higher chlorophyll concentration during NEM than SWM.

Our finding of the dominance of diatoms, in 2018-2019, is not consistent with previous reports which indicated the dominance of dinoflagellates in the coastal waters of Muscat during most of the year (Al-Hashmi et al., 2012, 2014, 2015, and 2017), although in some periods, a dominant role of diatoms has been reported (Al-Abri and Bryantseva, 2015). The presented results open up a new vision of the long-term changes of phytoplankton community observed in the Sea of Oman, over the past decade. This marked increase of diatoms stemmed from high concentrations of silicates observed in the region. This level was about four fold less during the previous decade (Al-Hashmi et al., 2015). All these episodes, compared with our current sampling, implied the seasonality of coastal phytoplankton community to be subjected to marked interannual variations caused by a regional circulation, which, in turn, affects the availability of nutrients. Stronger wind stress and current velocity lead to turbulent mixing causing high nutrient concentration at the sea surface. Regional circulation depends upon the location and intensity of mesoscale cyclonic and anticyclonic eddies in the Sea of Oman. Seasonal spatial shifts of these eddies drive the current velocity and their direction, as well as the vertical distribution of temperature, salinity, density and phytoplankton (Piontkovski et al., 2016).

Wind and geostrophic flow control SST by driving horizontal advection, vertical mixing and coastal upwelling At the onset of periods of lower than average SST in July-August 2018 and February-March 2019 (Figure 3) high abundance of phytoplankton were sampled (Figure 7). In late July and August 2018 a large intense anticyclonic eddy in the eastern central Sea of Oman advected cool upwelling water from the Arabian Sea towards northwest along the Omani coast between Sur and Muscat. This resulted in a reduction of the SST around Muscat compared to previous years and coincides with a peak in sampled phytoplankton. During well mixed winter conditions in late February and March 2019 the recorded SST dropped again significantly below the 9 year average mainly due to increased mixing by strong alternating wind. Again, the SST drop coincided with high sampled biomass in late February and March. The other potential factor is the eutrophication of coastal waters caused by the industrial impact. However, our sampling didn't involve the characteristics of industrial pollution.

Dactyliosolen fragilissimus and *Chaetoceros spp.* occurred in high numbers. The genus *Chaetoceros* was the common important dominate genus in Sohar and Muscat during winter in surface and 20 m depth while summer population composed of mixed benthic and centric diatoms. *Chaetoceros* contributed markedly to open nutrient-reach upwelled waters of the Sea of Oman, taken as a characteristic of high productive coastal system (Polikarpov et al., 2016). Therefore, the abundance of diatoms can be taken as indication of strong coastal upwelling and high primary productivity during the sampling periods. On the other hand, outside the upwelling seasons, diatom frequency decreased dramatically to the lowest abundance.

Diatoms were very diverse composing of 130 species including coastal and open water species, although the diversity could be higher, over years (Al-Abri and Bryantseva, 2015). The highest number of species and hence abundance (reaching bloom condition) were recorded during the NEM and SWM when nutrients were abundant. Stronger monsoon winds boost algae growth by bringing more nutrients from the deep ocean to the surface. The diatom population tends to be more diverse during bloom conditions than dinoflagellates as they functions more as a guild of complementing species (Smayda and Reynolds, 2003). The co-occurrence of more coastal species like *Pseudo-nitzschia spp.* and *Chaetoceros spp.* with more open water species *Nitzschia bicapitata* (occurring during SWM) indicates mixing of different nutrient rich water masses (Lange et al., 1994; Treppke et al., 1996).

The Sea of Oman region is subjected to a monsoonal mode of atmospheric processes. The Siberian High atmospheric pressure system, which is the anomaly defined by values above 1028 hPa over the middle to higher Asia continent, affects the region in winter (Kim et al., 2005). The South-west Monsoon affects the region from June through September, although temporal shifts of monsoonal periods were noticed (Loo et al., 2015). Monsoonal winds favor the enrichment of euphotic layer of the ocean with nutrients. In particular, silicates are the most important, for the proliferation of diatoms, while nitrates fuel dinoflagellate blooms (Dagenais-Bellefeuille and Morse, 2013; Smetacek, 1998). Regionally, we dealt with seasonal winds, as well as intra-seasonal variations of the wind speed and the impact of mesoscale eddies on the dynamics of nutrients and hence, the phytoplankton populations.

Al-Hashmi et al. (2014, 2015) carried out monthly sampling in a shallow (15m deep) Bandar Khayran Bay, near Muscat. The phytoplankton community was represented by 287 species, dominated by dinoflagellates. Similar sampling on a coastal station in the Sohar region showed that small flagellates and diatoms contributed 10 and 25% correspondently, to the phytoplankton abundance from January to April 2010 (Al Abri, 2013). The dominant genera of *Dinophytae* were *Prorocentrum*, *Gymnodinium* and *Dinophyta* while in March-2010 the dominant genera shifted to *Chaetoceros* and *Thalasiosira.* In March 2011, *Rhizosolenia* contributed more than 90% to phytoplankton followed by small flagellates. All these episodes, compared with our current sampling, implied the seasonality of coastal phytoplankton community to be subjected to marked inter-annual variations. On top of this, the situation with dominance could be different in offshore waters. For instance, the species of *Chaetoceros* contributed markedly to open nutrient-reach waters of the Sea of Oman,

in winter-2006, while *Pseudo-nitschia spp.* and *Skeletonema sp.* were the main bloom forming taxa in the central part of the Arabian Gulf (Polikarpov et al., 2016).

The comparison of remotely sensed chlorophyll-*a* in the Sea of Oman with a direct sampling of plankton, elucidated a good match, which implied the *Noctiluca* internally kept symbionts (dinoflagellates) to be the main contributors to the observed color, during blooms (Harrison et al., 2011). Linkages between *Noctiluca* and chlorophyll-*a* concentration have been reported over coastal and open ocean regions, in the Arabian Sea basin (Al-Hashmi et al., 2019; Gomes et al., 2008). Interestingly, the seasonality of *Noctiluca* peaks does not correspond to that of any other abundant phytoplankton species (Table 2).

To reproduce huge cells massively, the *Noctiluca* population needs high food supply. With this regard, many investigators reported a tight association of *Noctiluca* blooms with the diatom blooms (KiØrboe and Titelman, 1998; Dela-Cruz et al., 2002; Turkoglu, 2013), as well as the selective feeding on diatoms in cases of mixed diets, in experiments (Zhang et al., 2016). The comparison of monthly time series elucidated the phenomenon of the time lag of *Noctiluca* abundance with regard to abundance peaks of 20 other abundant phytoplankton species dominated by diatoms (Table 2). Presumably, the mechanism of this time lag is mediated by different growth rates of diatoms and *Noctiluca* and a variety of trophic interactions between *Noctiluca* (acting as the predator) and the phytoplankton species consumed by this predator. A periodic (seasonal) increase in diatoms leading to a delayed increase in *Noctiluca* was reported for the northern Arabian Sea (Dwivedi et al., 2016). Overall, the mixotrophic feeding behavior and in particular, a different predation pressure of *Noctiluca* on diatoms and dinoflagellates has been reported for a number of regions, worldwide (Kopuz et al., 2014; Sriwoon et al., 2008; 2011; Suzuki et al., 2013).

Monsoonal and regional winds play an important role in regulating algal blooms. This regulation was exemplified by introducing a three-dimensional diagram that approximated the concentration of remotely sensed chlorophyll-*a* (contributed by *Noctiluca* symbionts) as the function of zonal and meridional components of the wind speed (Figure 5). In general, it is believed that the wind-induced mixing of the upper layer is rather associated with the wind stress than the wind speed, although both characteristic are related (Kahru et al., 2010). Therefore it is implied that maximal values of chlorophyll-*a* is associated with peaks of zonal and meridional component of the wind stress. Retrospective analysis of 17 year monthly remotely sensed chlorophyll-*a* concentration in the Muscat region showed that the majority of peaks matched the time of the NEM. In comparing winter blooms in the Arabian Gulf with that in a deep Sea of Oman, we implied the spatial correlation of the wind speed with remotely sensed chlorophyll-*a* to be more pronounced in a shallow south-eastern part of the Arabian Gulf (Piontkovski et al., 2019).

An important role of winds in mediating *Noctiluca* bloom development has been noticed for the northern Adriatic Sea and the Black Sea (Mikaelyan et al., 2014). However, the authors elucidated a negative relationship between the number of cells in the peak period and the wind velocity. They hypothesized that the wind-induced

turbulence suppresses the feeding process.

One of characteristic features of tropical and subtropical waters of the Arabian Sea is a great diversity of trophically interacting phyto- and zooplankton species. In 2018-2019, in the Sea of Oman, in Muscat coastal waters, 79 copepod species were potential consumers of 249 phytoplankton species. Seasonal patterns of the abundance of potential predators and their prey were diverse and in general, exhibited lack of correlations on a seasonal scale. For instance, the matrix of correlations between six relatively abundant phytoplankton and copepod species gave no statistically significant cases, which point at uncorrelated seasonal fluctuations or at potential time lags in these correlations.

As far as zooplankton species diversity is concerned, we reported its increase, from the Arabain Gulf eastward-to the Gulf of Oman (Sea of Oman) and might extend this trend towards the open waters of the Arabian Sea in which number of copepod species exceeds 180 (Madhupratab and Haridas, 1986; Prusova et al., 2012; Sewell, 1947). An increase of copepod species abundance from coastal to open oceanic waters was reported for various regions of the Indian Ocean (Goswami and Padmavati, 1996; Mwaluma et al., 2003). Usually, an increase of copepod species diversity is accompanied by a declining biomass of zooplankton (Rakhesh at al., 2006).

A statistical analysis has indicated coupling of *Noctiluca* with the total zooplankton concentration (in which copepods dominate), as well as the concentration of a particular copepod species (Figure 12 and 13). A statistical coupling of *Noctiluca* with small-sized herbivorous copepods, observed in monthly time series, might be associated with the similarity of their feeding patterns. Three species (namely, *Acrocalanus longicornis, Clausocalanus furcatus, and Clausocalanus plumulosus*), which formed a statistical cluster with *Noctiluca*, all are fine-filter feeders (Razouls et al., 2019; Turner, 2004). *Oncaea clevei,* which was identified as the carnivore species in our Table 3, was associated with this group as well (Figure 12). However, *Noctiluca* is capable of consuming small onceids (Enomoto, 1956). In being competitors for food, *Noctiluca* and small-sized copepods could mitigate competition through the trophic niche separation. The grazing pressure of *Noctiluca* on the total phytoplankton, along the southwest coast of India, was found to be 2.8 folds higher than that of the small copepods. However, *Noctiluca* exhibited the highest selectivity of large phytoplankton cells, in comparison to copepods which fed on a small-sized fraction (Arunpandi et al., 2017).

The assessment of the number of trophically interacting phyto- and zooplankton species is ecologically important, in understanding the seasonality of the turnover rate of phytoplankton through zooplankton. On a basin scale, seasonal patterns of copepod species diversity are tightly related to the seasonality of primary production (Woodd-Walker et al., 2002). A trophic stress imposed by zooplankton is high; up to 50-70% of daily primary production is consumed, during North-east and South-west monsoon seasons, along the Omani shelf overlooking the Arabian Sea (Smith et al., 1998). With this regard, the ratio of the net primary production to the zooplankton biomass reflects the turnover rate of this production through zooplankton. It indicates the

intensity of organic matter flow per zooplankton biomass unit (Piontkovski et al., 2003; Vinogradov and Shushkina, 1987). Our pilot assessments showed that the turnover rate of the net primary production through zooplankton in the Sea of Oman is 3 to 39 times higher than in the south-eastern part of the Arabian Gulf (in February and June, respectively). Planktivorous fishes could be sensitive to elucidated gradients of this ratio. Partially, this could explain regional differences in sardine catches, which are 10 times higher in the Sea of Oman (Piontkovski et al., 2019).

CONCLUSIONS

Seasonal variations of abundance of over 190 phytoplankton species inhabiting coastal waters of the Sea of Oman revealed that unusual dominance of diatoms over dinoflagellates. This dominance was closely related to the prevailing weather condition and to the availability of nutrients, especially silicate. Local wind, sea surface temperature and to a lesser extent geostrophic flow, show distinct seasonal variations. Inter-annual variability mainly arises from the superposition of average seasonal cycles with unusual events in geostrophy and wind. Unusual geostrophic flow occurred in July-August 2018 and May 2019 and strong wind events where frequent in early 2019. This reflected in periods of lower than average SST and coincided with high samplings of phytoplankton abundance and unusual species distribution.

The dinoflagellate, *Noctiluca scintillans* continues to lead the list of bloom-forming species. The *Noctiluca* bloom development lags the peaks of all other abundant phytoplankton species. The seasonal pattern of *Noctiluca* experiences marked changes of the onset, magnitude and life time of winter and summer blooms, over years.

Copepods were the most abundant in the zooplankton fraction of plankton community. No seasonal changes were observed in the number of copepod species over seasons. Seasonal variations of the abundance of species exhibited one or two peaks (which varied regionally), in August and November. Peak magnitudes varied gradually over species- from few thousands to 15,000 individuals per cubic meter. The main seasonal difference of the trophic structure dealt with the number of carnivores, from genera *Labidocera, Sapphirina, Corycaeus*, and some others.

In 2018-2019, in Muscat coastal waters, 79 copepod species were potential consumers of 249 phytoplankton species. Seasonal patterns of the abundance of potential predators and their prey were diverse and exhibited lack of correlations on a seasonal scale, which point at potential time lags.

ACKNOWLEDGEMENTS

Acknowledgements. This work was supported by the SQU, grant CL/SQU-UAEU/18/04, IG/AGR/FISH/17/02, and UAEU grant 31S321. We thank Salim Al-Khusaibi, Harib Al-Habsi, Bader Al-Bawaiqi and Hajir Al Lawati for technical assistance with sampling and sample processing.

REFERENCES

[1] Al-Abri, N., 2013, Phytoplankton Taxonomy, Abundance and Composition. In: Assessment of Mesoscale Physical-Biological Interactions along the coast of Oman as the Basis for Understanding the Periodic Fisheries losses. Final Report on Research Project: Ministry of Agriculture and Fisheries Wealth and Sultan Qaboos University. Muscat, pp.1-188.

[2] Al-Abri, N.M., Bryantseva, Yu.V., 2015, Diversity of the phytoplankton in the coastal waters of Oman (Arabian Sea). *Scientific notes of Volodymyr Hnatiuk Ternopil National Pedagogical University*. Series: Biology. Special Issue: Hydroecology, 64, 3-4, pp.779-783.

[3] Al-Hashmi, K., 2017, Marine hytoplankton guide of Oman's waters. *Oman Animal and Plant Genetic Resources Center*. Muscat, 184pp.

[4] Al-Hashmi, K.A., Sarma, Y.V.B., Claereboudt, M., Al-Azri, A.R., Piontkovski, S.A., 2012, Phytoplankton Community Structure in the Bay of Bandar Khyran, Sea of Oman with Special Reference to Harmful Algae. *International Journal of Marine Science*, 2, 5, pp.31-42.

[5] Al-Hashmi, K., Goes, J., Claereboudt M., Piontkovski, S.A., Al-Azri A., Smith S., 2014, Variability of dinoflagellate and diatoms in the surface waters of Muscat, Sea of Oman: comparison between enclosed and open ecosystem. *International Journal of Oceans and Oceanography*, 8, 2, pp.137-152.

[6] Al-Hashmi, K., Smith, S., Claereboudt, M., Piontkovski, S.A., Al-Azri, A., 2015, Dynamics of potentially harmful phytoplankton in a semi enclosed bay in the Sea of Oman. *Bulletin of Marine Science*, 91, pp.141-166.

[7] Al-Hashmi, K.A., Sarma, V.V.B., Piontkovski, S.A., Al-Habsi, H., Harrison P. J., 2019, Response of phytoplankton to changes in hydrographic properties in a subtropical embayment in the Sea of Oman. *International Journal of Ecology and Enrironmental Sciences*, 45, pp.71-84.

[8] Al-Azri, A.R., Piontkovski, S.A., Al-Hashmi, K., Goes, J.G., Gomes, H.D.R., 2010, Chlorophyll a as a measure of seasonal coupling between phytoplankton and the monsoon periods in the Gulf of Oman. *Aquatic Ecology*, 44, pp.449-461.

[9] Al-Yamani, F., Saburova, M.A., 2019a, Marine phytoplankton of Kuwait's waters. Diatoms. Volume II. Kuwait, 337p.

[10] Al-Yamani, F., Saburova, M.A., 2019b, Marine phytoplankton of Kuwait's waters. Cyanobacteria, Dinoflagellates, Flagellates. Volume I. Kuwait, 468p.

[11] Arunpandi, N., Jyothibabu, R., Jagadeesan, L., Gireeshkumar, T.R., Karnan, C., A.Naqvi, S.W., 2017, Noctiluca and copepods grazing on the phytoplankton community in a nutrient-enriched coastal environment along the southwest coast of India. *Environmental Monitoring and Assessment*, 189, 351, doi: 10.1007/s10661-017-6061-9.

[12] Brand, L.E., Guillard, R.L., 1981, The effects of continuous light and light

intensity on the reproduction rate of twenty-two species of marine phytoplankton. *Journal of Experimental Marine Biology and Ecology*, 50, pp.119-132.

[13] Chen, M., Kim, D., Liu H., Kang C-K., 2018, Variability in copepod trophic levels and feeding selectivity based on stable isotope analysis in Gwangyang Bay of the southern coast of the Korean Peninsula. *Biogeosciences*, 15, pp.2055-2073.

[14] Dagenais-Bellefeuille, S., Morse, D., 2013, Putting the N in dinoflagellates. *Frontiers in Microbiology*, 4, 369, doi:10.3389/fmicb.2013.00369.

[15] Dela-Cruz, J., Ajani, P., Lee, R., Pritchard, T., Suthers, I., 2002, Temporal abundance patterns of the red tide dinoflagellate Noctiluca scintillans along the southeast coast of Australia. *Marine Ecology Progress Series*, 236, pp.75-88.

[16] Dwivedi, R., Rafeeq, M., Sanjeevan, V.N. Sudhakar, M., 2016, Remote sensing of evolution and coupling of green Noctiluca and diatom blooms in the northern Arabian Sea using value-added time-series products. *Journal of Marine Biological Association of India*, 58, 2, pp.12-22.

[17] Enomoto, Y., 1956, On the occurrence and the food of Noctiluca scintillans (Macartney) in the waters adjacent to the west coast of Kyushu, with special reference to the possibility of the damage caused to the fish eggs by that plankton. *Bulletin of the Japan Society of Scientific Fisheries*, 22, pp.82-88.

[18] Fisheries Statistics Book, 2016, Ministry of Agriculture and Fisheries Wealth. Sultanate of Oman. Muscat, 246pp.

[19] Fisheries Statistics Book, 2018, Ministry of Agriculture and Fisheries Wealth. Sultanate of Oman. Muscat, 240pp.

[20] Glibert, P., 2007, Eutrophication and harmful blooms: a complex global issue, examples from the Arabian Sea including Kuwait Bay, and an introduction to the global ecology and oceanography of harmful algal blooms (GEOHAP) programme. *International Journal of Oceans and Oceanography*, 2, pp.157-169.

[21] Gomes, H.R., Goes, J.I., Matondkar, S.G., Parab, S.G., Al-Azri, A., Thoppil, P.G., 2008, Blooms of Noctiluca miliaris in the Arabian Sea-An in situ and satellite study. *Deep Sea Research*, Part I, 55, pp.751–765.

[22] Goswami, S.C., Padmavati, G., 1996, Zooplankton production, composition and diversity in the coastal waters of Goa. *Indian Journal of Marine Sciences*, 25, pp.91-97.

[23] Hankin, S., Davison, J., Callahan, J., Harrison, D. E., O'Brien, K., 1998, A configurable web server for gridded data: a framework for collaboration. In 14th International Conference on Interactive Information and Processing Systems for Meteorology, Oceanography, and Hydrology, *AMS*, pp.417-418.

[24] Harrison, P.J., Piontkovski, S.A., Al-Hashmi, K.A.,2019, Overview of decadal ecosystem changes in the Western Arabian Sea and the occurrence of algal

blooms. *Journal of Agricultural and Marine Sciences*, 23, pp.11–23.

[25] Kahru, M., Gille, S.T., Murtugudde, R., Strutton, P.G., Manzano-Sarabia, M., Wang, H., Mitchell, B.G., 2010, Global correlations between winds and ocean chlorophyll. *Journal of Geophysical Research*, 115, C12040, doi:10.1029/2010JC006500.

[26] Kim, D.W., Byun, H.R., Lee, Y.I., 2005, The long-term changes of Siberian High and winter climate over the northern hemisphere. *Journal of Korean Meteorologic Society*, 41, pp.275-283.

[27] KiØrboe, T., Titelman, J., 1998, Feeding, prey selection and prey encounter mechanisms in the heterotrophic dinoflagellate Noctiluca scintillans. *Journal of Plankton Research*, 20, 8, pp.1615-1636.

[28] Kleppel, G.S., 1993, On the diets of calanoid copepods. *Marine Ecology Progress Series*, 99, pp.183-195.

[29] Kopuz, U., Feyzioglu, A.M., Valente, A., 2014, An unusual red tide event of Noctiluca Scintillans (Macartney) in the southeastern Black Sea. *Turkish Journal of Fisheries and Aquatic Sciences*, 14, pp.261-268.

[30] Lange, C.B., Treppke, U.F., Fischer, G., 1994, Seasonal diatom fluxes in the Guinea basin and their

[31] relationships to trade winds, hydrography and upwelling events. *Deep-Sea Research*, 41, pp.1843-1860.

[32] L'Hégaret, P.L., Duarte, R., Carton, X., Vic, C., Ciani, D., Baraille, Corréard, S., 2015, Mesoscale variability in the Arabian Sea from HYCOM model Results and observations: impact on the Persian Gulf Water path. *Ocean Science*, 11, pp.667-693.

[33] Longhurst, A., 1998, Ecological geography of the sea. *Academic Press.* San Diego, 398pp.

[34] Loo, Y.Y., Billa, L., Singh, A., 2015, Effect of climate change on seasonal monsoon in Asia and its impact on the variability of monsoon rainfall in Southeast Asia. *Geoscience Frontiers*, 6, 6, pp.817-823.

[35] Mackas, D.L., Greve, W., Edwards, M., Chiba, S., Tadokoro, K., Eloire, D., Mazzocchi, M.G., Batten, S., Richardson, A.J., Johnson, C., Head, E., Conversi, A., Peluso, T., 2012, Changing zooplankton seasonality in a changing ocean: comparing time series of zooplankton phenology. *Progress in Oceanography*, 97-100, pp.31-62.

[36] Madhupratab, M., Haridas, P., 1986, Epipelagic calanoid copepods of the northern Indian Ocean. *Oceanologica Acta*, 9 pp.105-117.

[37] Mikaelyan, A., Malej, A., Shiganova, T., Turk, V., Sivkovitch, A.E, Musaeva, E., Kogovšek, T., Lukasheva, T., 2014, *Harmful Algae*, 33, pp.29-40.

[38] Mwaluma, J., Ozore, M., Kamau, J., Wawiye, P., 2003, Composition,

abundance and seasonality of zooplankton in Mida Kreek, Kenya. Western Indian Ocean *Journal of Marine Science,* 2, 2, pp.147-155.

[39] Nogueira, E., González-Nuevo, G., Valdés,L., 2012, The influence of phytoplankton productivity, temperature and environmental stability on the control of copepod diversity in the North East Atlantic. *Progress in Oceanography*, 97-100, pp.92-107.

[40] Piontkovski, S.A., Williams, R., Ignatyev, S., Boltachev, A., Chesalin, M., 2003, Structural-functional relationships in the pelagic community of the eastern tropical Atlantic Ocean. *Journal of Plankton Research,* 25, pp.1021-1034.

[41] Piontkovski, S.A., Queste, B., Al-Shaaibi, A., Al-Hashmi, K., Bryantseva, J., Popova, E., 2016, Subsurface algal blooms of the north-western Arabian Sea. *Marine Ecology Progress Series*, 566, pp. 67-78.

[42] Piontkovski, S.A., Hamza, W., Al-Abri, N., Al-Busaid,i S., Al-Hashmi, K.A., 2019, A comparison of seasonal variability of Arabian Gulf and the Sea of Oman pelagic ecosystems. *Aquatic Ecosystem Health and Management*, 22, pp.108-130.

[43] Polikarpov, I., Saburova, M., Al-Yamani, F., 2016, Diversity and distribution of winter phytoplankton in the Arabian Gulf and the Sea of Oman. *Continental Shelf Research*, 19, pp.85-99.

[44] Prusova, I., Smith, S., Popova, E., 2012, Calanoid Copepods of the Arabian Sea Region. *Sultan Qaboos University Academic Publication Board*, Muscat, Sultanate of Oman, 240 pp.

[45] Quinn, N.J., Johnson, D.W., 1996, Cold water upwelling cover Gulf of Oman. Coral Reefs, pp.15-214.

[46] Rakhesh, M., Raman, A.V., Sudarsan, D., 2006, Discriminating zooplankton assemblages in neritic and oceanic waters: a case for the northeast coast of India, Bay of Bengal. *Marine Environmental Research*, 61, pp.93-109.

[47] Razouls, C., de Bovée, F., Kouwenberg, J., Desreumaux, N., 2019, Diversity and geographic distribution of marine planktonic copepods. *Sorbonne University*, CNRS. http://copepodes.obs-banyuls.fr/en [Accessed October 7, 2019].

[48] Raymont, J.E.G., 1980, Plankton and productivity in the oceans. *Pergamon Press.* Oxford, 477pp.

[49] Reynolds, C. S., 2006, Ecology of Phytoplankton. Cambridge: *Cambridge University Press*, doi: 10.1017/CBO9780511542145.

[50] Richen, M.L., Morton, S.L., Jamali, E.A., Rajan, A., Anderson, D.M., 2010, The catastrophic 2008-2009 red tide in the Arabian Gulf region, with observations on the identification and phylogeny of the fish-killing dinoflagellate *Cochlodimium polykrikoides*. *Harful Algae*, 9, pp.163-172.

[51] Round, F.E., 1990, The diatoms: biology and morphology of the genera. *University Press.* Cambridge.

[52] Sewell, R.B., 1947, The free-swimming planktonic Copepoda. Systematic account. *Scientific Report. John Murray Expedition*, 8, pp.1-303.

[53] Skalar Analytical, 1996, Operating Manual. *Skalar Analytical* B.V.Breda, The Netherlands.

[54] Smayda, T. J., Reynolds, C. S., 2003, Strategies of marine dinoflagellate survival and some rules of assembly. *Journal of Sea Research,* 49, pp.95–106.

[55] Smetacek, V., 1998, Diatoms and the silicate factor. *Nature*, 391, pp.224-225.

[56] Smith, S., Roman, M., Prusova, I., Wishner, K., Gowing, M., Codispoti, L., Barber, R., Marra, J., Flagg, C., 1998, Seasonal response of zooplankton to monsoonal reversals in the Arabian Sea. *Deep-Sea Research* II, 45, pp.2369-2403.

[57] Sriwoon, R., Pholpunthin, P., Lirdwitayaprasit, T., Kishino, M., Furuya, K., 2008, Population dynamics of green Noctiluca scintillans (Dinophyceae) associated with the monsoon cycle in the upper Gulf of Thailand. *Journal of Phycology*, 44, pp.605-615.

[58] Sournia, A., 1986, Atlas du phytoplankton marin, cyanophyceae, dictyochophyceae, dinophyceae et raphidophyceae. Vol,1. I. Paris: Editions CNRS.

[59] Suzuki, T., Yamomoto, K., Narasaki, T., 2013, Predation pressure of Noctiluca scintillans on diatoms and thecate dinoflagellates off the western coast of Kyushu, Japan. *Plankton and Benthos Research,* 8, 4, pp.186-190.

[60] Treppke, U.F., Lange, C.B., Donner, B., Fischer, G., Ruhland, G., Wefer, G., 1996, Diatom and silicoflagellate fluxes at the Walvis Ridge: an environment influenced by coastal upwelling in the Benguela System. *Journal of Marine Research*, 54, pp.991-1016.

[61] Tomas, C.R., 1997, Identifying Marine Phytoplankton. *Academic Press,* San Diego, California.

[62] Turkoglu, M., 2013, Red tides of the dinoflagellate *Noctiluca scintillans* associated with eutrophication in the Sea of Marmara (the Dardanelles, Turkey). *Oceanologia*, 55, 3, pp.709-732.

[63] Turner, J.T., 1984, The feeding ecology of some zooplankters that are important prey items of larval fish. *NOAA Technical Report*, NMFS-7, pp.1-28.

[64] Turner, J.T., 2004, The importance of small planktonic copepods and their roles in pelagic marine food webs. *Zoological Studies*, 43, pp.255-266.

[65] Vinogradov, M.E., Shushkina, E.A., 1987, The functioning of the plankton communities of the ocean epipelagic (Funkcionirovanie planktononnyih soobchest epipelagiali okeana). *Nauka,* Moscow, 240pp (in Russian).

[66] Warwick, R.M., Clarke, K.R., 1991, A comparison of some methods of analysing changes in benthic community structure. *Journal of the Marine Biological Association of the United Kingdom*, 71, pp. 225-244.

[67] Woodd-Walker, R., Ward, P., Clarke, A., 2002, Large-scale patterns in diversity and community structure of surface water copepods from the Atlantic Ocean. *Marine Ecology Progress Series*, 236, pp.189-203.

[68] Zhang, S., Liu, H., Guo, C., Harrison, P., 2016, Differential feeding and growth of *Noctiluca scintillans* on monospecific and mixed diets. *Marine Ecology Progress Series*, 549, pp.27-40.